Current Osteoporosis Reports (2020) 18:57–66
https://doi.org/10.1007/s11914-020-00562-x

IMAGING (F. WEHRLI AND T. LANG, SECTION EDITORS)

MRI Assessment of Bone Marrow Composition in Osteoporosis

Xiaojuan Li[1] · Ann V. Schwartz[2]

Published online: 18 January 2020

Abstract

Purpose of Review To provide an overview on recent technical development for quantifying marrow composition using magnetic resonance imaging (MRI) and spectroscopy (MRS) techniques, as well as a summary on recent findings of interrelationship between marrow adipose tissue (MAT) and skeletal health in the context of osteoporosis.

Recent Findings There have been significant technical advances in reliable quantification of marrow composition using MR techniques. Cross-sectional studies have demonstrated a negative correlation between MAT and bone, with trabecular bone associating more strongly with MAT than cortical bone. However, longitudinal studies of MAT and bone are limited. MAT contents and composition have been associated with prevalent vertebral fracture. The evidence between MAT and clinical fracture is more limited, and, to date, no studies have reported on the relationship between MAT and incident fracture.

Summary Increasing evidence suggests a dynamic role of marrow fat in skeletal health. Reliable non-invasive quantification of marrow composition will facilitate developing novel treatment strategies for osteoporosis.

Keywords Bone marrow composition · Marrow adipose tissue · Bone marrow fat · Bone-fat interaction · Osteoporosis · Marrow MR

Introduction

Bone marrow, the primary site of hematopoiesis, is one of the largest organs in the body that accounts for up to 4–5% body weight. Marrow tissue is composed primarily of hematopoietic cells, adipocytes, and supportive stromal cells surrounded by vascular sinuses and trabecular bone. Marrow composition changes dynamically with altered hematopoietic needs, resulting from aging, pathologies, and other factors. The well-known conversion from "red" to "yellow" marrow continues throughout life following a pattern from the peripheral toward the central skeleton. Historically, marrow fat increasing with age has been viewed as a neutral process, with marrow adipose tissue (MAT) serving as a "space filler" in the bone marrow. Emerging evidence suggests that MAT is a distinct fat depot with different properties and functions from other fat depots, and plays a dynamic role affecting both bone quantity and quality (1, 2). The mechanism of this bone-fat interaction, however, is not fully understood (3, 4). Hypotheses include allocation shift of mesenchymal stem cells from the osteoblast lineage toward the adipocyte lineage (5, 6) (although the definitive lineage of marrow adipocytes remains largely unknown and controversial), and potential direct impact on bone turnover by secreting an array of factors with autocrine and paracrine effects (7–9).

In parallel of figuring out the underlying mechanism of bone-fat interaction, there is an increasing interest of quantifying bone marrow composition using non-invasive imaging, which will enable large-scale human subject studies and facilitate development of novel therapeutic strategies for osteoporosis with marrow fat severing as a novel treatment target. This review will discuss recent developments in quantitative MRI assessment of bone marrow composition, including water-fat MR imaging, MR spectroscopy, diffusion and perfusion MRI, followed by recent findings of interrelationship between MAT and skeletal health of human subjects in the context of osteoporosis.

This article is part of the Topical Collection on *Imaging*

✉ Xiaojuan Li
Lix6@ccf.org

[1] Department of Biomedical Engineering, Program of Advanced Musculoskeletal Imaging (PAMI), Cleveland Clinic, 9500 Euclid Avenue, ND20, Cleveland, OH 44195, USA

[2] Department of Epidemiology and Biostatistics, University of California, San Francisco, CA, USA

MR Techniques for Bone Marrow Composition Measurement

MR Imaging and Spectroscopy for Quantifying Marrow Adipose Tissue

Water-Fat MRI

MRI provides high-resolution 3D images with superior contrast of soft tissues and without ionizing radiation. Clinically, T1-weighted images without fat suppression, and fat-suppressed or fluid-sensitive T2-weighted images, have been used widely for visualizing bone marrow lesions (10–12). T1-weighted MRI has also been used to quantify MAT volume based on thresholding methods (13), which however is limited by potential bias introduced by MR signal variability. Chemical shift-encoding-based water-fat MRI (Dixon-MRI or CSE-MRI) has been developed and applied in bone marrow to provide superior fat suppression as well as "absolute" and standardized proton density fat fraction (PDFF) maps (14, 15).

The initial 2-point Dixon method (16) suffers from assuming perfect B_0 homogeneity while Dixon imaging with 3 or more echoes takes into account field inhomogeneity and other co-founding factors (17). In Dixon methods, separate water and fat images are generated based on parameter estimation using either complex or magnitude signals (normally vendors also provide in-phase and out-of-phase images). Methods based on complex images have the advantage of better noise performance and lower sensitivity to fat signal modeling errors compared with magnitude-based methods. However, complex-based methods are also more prone to phase errors induced by hardware imperfections including concomitant gradients, eddy currents, and gradient delays (18–21). In addition to phase errors, other co-founding factors that need to be considered to minimize bias on PDFF estimate include the presence of multiple peaks in the fat spectrum, presence of susceptibility-induced fat resonance shifts, T_2* effects, and T_1 effects (22–26•).

MAT quantification using Dixon imaging were reported to significantly correlate with measures from dual source CT (DECT) ($r = 0.88$) and histology ($r = 0.772$) (27), and MR spectroscopy (26•, 28). A specimen study reported strong correlation between the known fat fraction and PDFF measured by 6-point Dixon imaging and iterative decomposition of fat and water with echo asymmetry and least squares estimation (IDEAL) reconstruction ($R^2 = 0.97$). However, a small systematic underestimate (− 3.2%) by IDEAL PDFF was observed. The authors suggested that, although difficult, signal modeling allowing for independent correction of T_2* for the different fat components as well as water might be useful toward more accurately estimating PDFF in the presence of trabecular bone (29).

Excellent in vivo reproducibility was reported for MAT quantification using water-fat MRI: coefficients of variation (CVs) were 1.7%, 3.0%, and 4.8% for repeated scans on the same day with repositioning, 6 weeks and 6 months apart, respectively (30, 31), and intra-class correlation coefficients (ICC) > 0.97 for repeated scans 2 weeks apart (32, 33•). A recent study involving both 1.5T and 3T scanners from two vendors reported high linearity ($r^2 = 0.972$–0.978) and small mean bias (0.6–1.5%) with 95% limits of agreement within 3.4% of PDFF of lumber vertebral bodies across field strengths, imaging platforms, and readers (33•).

MR Spectroscopy

MR spectroscopy (MRS) has been considered as the gold standard for quantifying MAT contents and composition. MRS studies in bone marrow have used primarily single voxel spectroscopy (SVS), which were acquired by either point-resolved spectroscopy (PRESS) or stimulated echo acquisition mode (STEAM). STEAM has several advantages over PRESS. First, STEAM allows shorter minimal TE, hence leading to less T2 weighting of the signal. Second, by using 90° pulses only (PRESS uses 90° followed by two 180° pulses), STEAM can provide sharper slice profile, and higher bandwidth which results in less chemical shift displacement artifact of the selected volume. Lastly, it was suggested that STEAM was less affected by J-coupling effects than PRESS, and consequently less prone to T2 underestimate and fat peak area overestimation (34). However, the major drawback of STEAM is that it provides only 50% SNR compared with PRESS at given TR and TE.

Figure 1 shows a typical MR spectrum collected in the vertebrae on clinical scanners. Based on peak assignment from high-resolution NMR spectroscopy in acylglycerol mixtures and MAT samples (35–37), lipid peaks I, IV, V, and VI are assigned to resonances of lipid protons at 0.90 ppm, 2.77 ppm, 4.20 ppm, and 5.31 ppm respectively. Peak II is assigned to the superposition of resonances at 1.30 ppm and 1.59 ppm, and peak III is assigned to the superposition of resonances at 2.03 ppm and 2.25 ppm. The water peak is at 4.7 ppm. From these peaks, two parameters can be derived to characterize the marrow fat:

$$\text{Fat Content (FC)} = \text{All lipids}/(\text{All lipids} + \text{water})*100\% \quad (1)$$

$$\text{Unsaturation Index (UI)} = \text{Unsaturated Lipids (5.3 ppm)}/\text{All Lipids}*100\% \quad (2)$$

The in vivo MRS data analysis for accurate fat quantification in bone marrow, especially fat composition, is

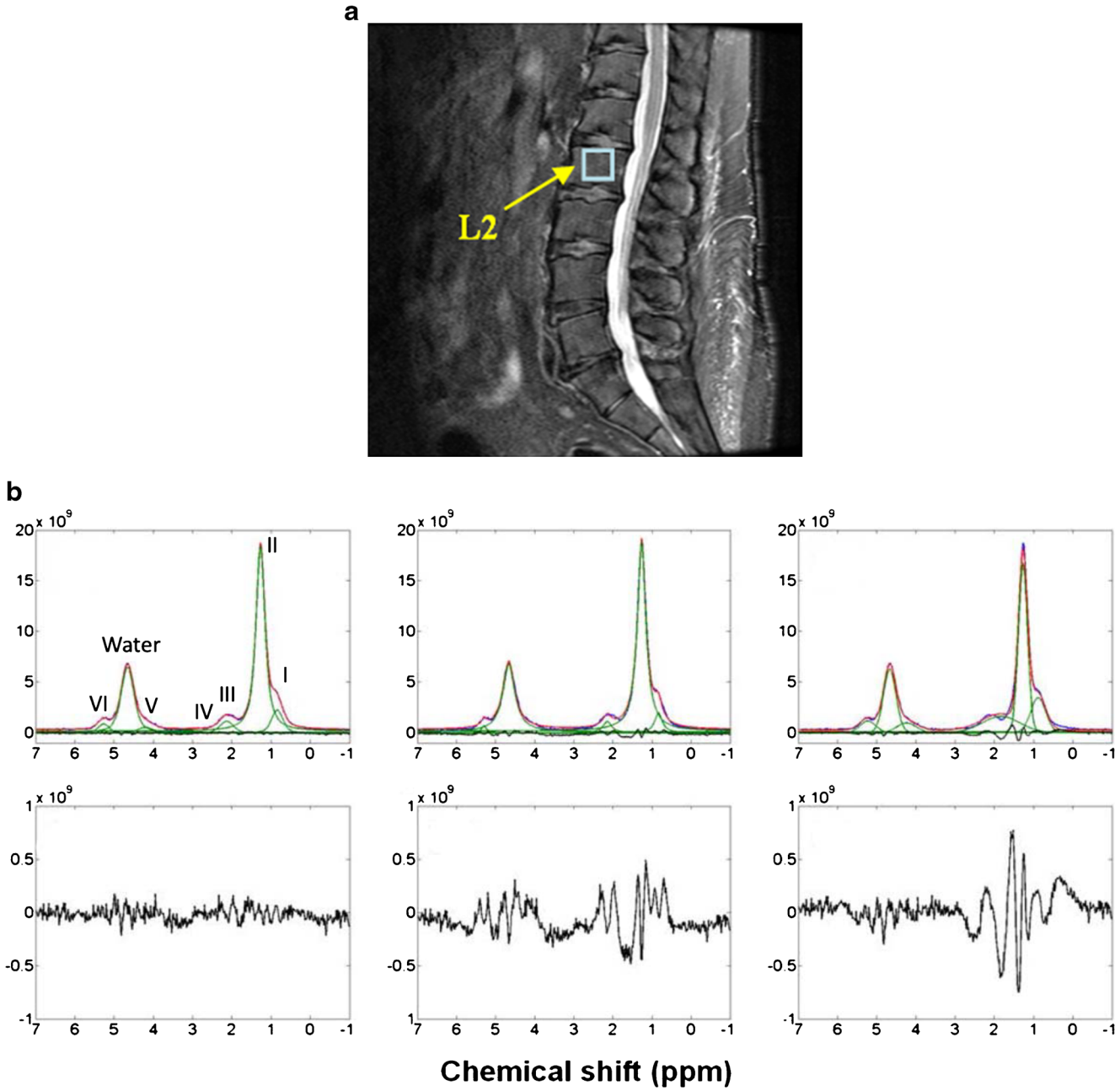

Fig. 1 **a** Single voxel MRS data in L2 using PRESS sequence at 1.5 Tesla (female, 92 years old). **b** Lipid peaks I, IV, V, and VI were assigned to resonance of lipid protons at 0.90 ppm [–$(CH_2)_n$–CH_3)], 2.77 ppm [–CH=CH–CH_2–CH=CH–], 4.20 ppm [–CH_2–O–CO–], and 5.31 ppm [–CH=CH–], respectively. Peak II was assigned to the superposition of resonances at 1.30 ppm [–$(CH_2)_n$–] and 1.59 ppm [–CO–CH_2–CH_2–], and peak III was assigned to the superposition of resonances at 2.03 ppm [–CH_2–CH=CH–CH_2–] and 2.25 ppm [–CO–CH_2–CH_2–]. The water peak was at 4.7 ppm. The spectrum was fitted using Voigt model (left column), pure Lorentzian model (middle column), and pure Gaussian model (right column). Blue, red, and green curves represent the experimental spectrum, the fitting spectrum, and the spectra of separated components, respectively. Fitting residuals are plotted in black and enlarged in bottom row (adapted from reference (48))

challenging due to line broadening caused by susceptibility differences between bone and marrow, and superposition of spectral peaks. Peak area integration has been used, which however has limited capability of quantifying overlapping peaks (38–40). Peak fitting methods using LC models with pre-defined base-sets (41, 42) or using line-shape models with prior information in either frequency-domain (26•, 43, 44) or time-domain (45, 46) can help to improve the quantification accuracy. Previous studies with line-shape model fitting mostly used Lorentzian or Gaussian models for the fitting. A recent study showed that using Voigt model reduced the fitting error by 33.8% and 32.3% compared with using Lorentzian and Gaussian models respectively (47) (Fig. 1b). Using Voigt models and time-domain fitting, a fully automatic algorithm

was developed with high reliability and repeatability of quantifying MAT contents and composition even for data collected at 1.5 Tesla (47). Other factors affecting fat contents or composition evaluation include the different T_2 weights of water and lipids in spectrum acquired with single TE. Acquiring data with multiple TEs will allow T_2 correction (48•).

In vertebral bodies, the CVs of FC were reported to range from 1.5 to 5.9% for rescans on the same day with repositioning between scans (43, 47, 49). The ICCs were 0.97 and 0.95 and CVs were 9.9% and 12.3% for repeated scans at 6 weeks and 6 months respectively (50). In femur, the ICCs were 0.78–0.85 for repeated scan within a week (51), or CV of 5% within 10 days (41). UI normally has inferior repeatability compared with FC, with CV reported to range from 5.1 to 10.7% for scans on the same day with repositioning between scans (43, 47). The reliability of UI estimate depends on both the spectral SNR and spectral resolution (47). High field strength will help to improve both aspects. Studies reported that FC increases significantly from L1 to L4 (39, 43, 47), while UI has no such trend (47).

Compared with MRS, water-fat MRI has the advantages of higher spatial resolution, which is valuable especially in areas with heterogeneous marrow distribution. However, it is more challenging to quantify marrow fat composition accurately using water-fat MRI. Water-fat MRI or CSE-MRI that can simultaneously quantify fat contents and composition has been developed, initially in liver (52, 53•). The feasibility of applying this technique in bone marrow has been shown recently (54, 55); however, more validation is warranted in the trabecularized marrow. On the other hand, with recent algorithm developments, in vivo MRS showed excellent reliability of quantifying different fat components in marrow. However, SVS has limited coverage and only average measures over the whole volume are available. MR spectroscopic imaging (MRSI) can provide spatially resolved assessment (although normally still at a lower resolution than water-fat MRI). The feasibility of bone marrow MRSI was shown in the knee (56), and more work is needed for evaluating osteoporosis in spine and other sites.

Perfusion and Diffusion MRI in Bone Marrow

Perfusion and diffusion MRI are established quantitative MR techniques that have been applied in bone marrow for characterizing tumors and metastases, metabolic diseases, osteoporosis, and fractures (15, 57, 58).

Perfusion MRI measures tissue hemodynamics, and perfusion MRI studies in bone marrow have been primarily performed using dynamic contrast-enhanced (DCE) MRI. T_1-weighted MR images are acquired before, during, and after rapid intravenous injection of Gd-based contrast agents that shorten T_1 when the bolus passes through the tissue. Perfusion parameters, including maximum enhancement, slope, and transit time, can be extracted from the perfusion time-signal curve, using empirical quantitative methods. To obtain more machine-independent parameters that are physiologically meaningful, including blood volume, flow, transit time constants, and permeability, tracer kinetic modeling has been applied with the requirement of an arterial input function (AIF). In femur, CVs of MR perfusion (scan and rescan at 1 week) ranged from 0.59 (enhancement slope femoral head) to 0.98 (enhancement maximum acetabulum) (51). Decreased perfusion was observed with decreased BMD in vertebral body (45, 59, 60) and in femur (61, 62). Furthermore, femur perfusion parameters (and marrow fat) at baseline predicted bone loss in femoral neck over 4 years (63). However, the effect of fat signal on perfusion parameter quantification needs to be addressed (64•, 65). Despite interesting results, the usage of contrast agent has impeded wide applications of perfusion MRI for studying osteoporosis.

Diffusion MRI is sensitive to Brownian motion, or "self-diffusion" of water molecule that is related to tissue microstructure and organization by using an additional pair of diffusion-weighting or dephasing gradient pulses into existing pulse sequences. Diffusion MRI based on single-shot echo-planar imaging (ssEPI) is the most commonly used sequences due to its fast acquisition and robustness to motion. However, applying ssEPI-diffusion MRI in bone marrow is challenging due to the susceptibility difference between bone and marrow and the images are prone to geometric distortions especially at high resolution. Methods to reduce such distortions include using reduced-FOV EPI, single-shot turbo-spin-echo or fast-spin-echo, and steady-state free-precession sequences showed promising results in bone marrow applications (58). Apparent diffusion coefficients (ADCs) of normal vertebral bone marrow were reported to range between 0.2 and 0.6×10^{-3} mm^2/s, which is lower than almost all other tissues except fat in human body (58). The slow diffusion demands large diffusion weight which however will result in low SNR. Marrow ADC were reported to decrease from L1–L5 (66) and decrease with increasing age (67, 68), which may be explained by increased marrow fat from L1–L5 and with increasing age thus more restriction to the water diffusion. However, it should be noted that, because fat has very low diffusion, data acquisition without fat suppression or with less optimal fat suppression will result in underestimates of marrow ADC (65).

A number of studies reported decreased ADC with decreased BMD (67, 69, 70); other studies reported either no correlation between ADC and BMD (60), or even a slight increase of ADC with decreased BMD (71). The different results between studies may be explained by different diffusion sequences and parameters, post-processing methods, and study cohorts. In general, to accurately quantify marrow water diffusion is technically challenging (susceptibility inhomogeneity, low diffusion, requirement for optimal fat suppression). More technical development and clinical evaluations are

needed to define the clinical values of diffusion MRI to evaluate and monitor marrow composition in osteoporosis.

Marrow Adipose Tissue and Skeletal Health

Marrow Fat and Bone

An early study reported an association between increased MAT and osteoporosis, using biopsy assessments of marrow composition (72). The availability of non-invasive measurements of marrow adiposity has allowed an expansion of research into associations with bone. A range of studies have reported a cross-sectional relationship between higher MAT and lower bone density, measured with dual x-ray absorptiometry (DXA) (45, 49, 60, 73, 74). For example, studies in Hong Kong reported that average MAT was 68% versus 59% in women and 58% versus 50% in men, for those with osteoporosis and normal BMD, respectively, based on spine BMD by DXA (45, 46, 47, 60).

BMD measured by DXA is central to clinical assessment of fracture risk, but QCT measures of bone have important advantages for research, including a volumetric bone density (vBMD) measurement, ability to distinguish cortical and trabecular bone, and estimates of bone strength parameters. As with DXA measures of aBMD, lower vBMD by QCT is associated with increased MAT (49, 75–78). Trabecular bone appears to be more strongly associated with MAT than cortical bone. In a cohort of older adults in Iceland, higher MAT was associated with lower levels of trabecular vBMD at the spine, total hip, and femoral neck, but was not significantly associated with cortical vBMD at total hip or femoral neck in women (49). For example, for a 1 SD increase in MAT (+ 8%), older women had 4.0% (95% CI − 7.6 to − 0.1%) lower trabecular vBMD and only 0.5% (95% CI − 1.7 to 0.7%) lower cortical vBMD at the total hip. Negative correlations between MAT and vBMD have also been reported in obese patients measured prior to bariatric surgery (76, 77).

A limitation of these studies, which have used single energy (SE) QCT to assess the association between vBMD and MAT, is the artifact introduced by partial volume averaging, resulting in lower vBMD measurement due to bone voxels that contain fat. Thus, higher MAT artificially lowers SE QCT measurements of bone (78–80). The effects appear to be larger for trabecular versus cortical vBMD. A recent study assessed the effect of this artifact by comparing results using SE QCT and dual energy (DE) QCT which is less confounded by marrow fat levels. This study of 129 early postmenopausal women recruited at the Mayo Clinic reported that SE QCT underestimates bone compared with DE QCT by 17.6% for trabecular spine vBMD but only 3.2% for cortical femoral neck vBMD (78). In spite of this underestimation, the correlations between MAT, measured with DE QCT, and the two different estimates of vBMD, by SE QCT and by DE QCT, appeared similar. The correlation coefficient for the association between femur MAT and total vBMD was − 0.33 for both SE QCT and DE QCT. For trabecular spine vBMD, the correlations with femur MAT were − 0.28 for SE QCT and − 0.29 for DE QCT; correlations with spine MAT were − 0.57 for SE QCT and − 0.56 for DE QCT.

High-resolution peripheral QCT (HR-pQCT) provides measurements of bone microarchitecture but is currently only available at distal sites. To date, one study of marrow fat and HR-pQCT has been published (81). In a study of young adults with anorexia ($N = 47$) and healthy controls ($N = 55$), total vBMD at the distal radius was negatively correlated with vertebral MAT ($r = -0.35$, $p = 0.03$), measured by MRS. The negative correlation was limited to trabecular vBMD ($r = -0.30$, $p = 0.05$) and not evident for cortical vBMD ($r = -0.10$, $p = 0.51$). Stiffness of the distal radius, assessed with finite element analysis, was also negatively correlated with MAT (-0.37, $p = 0.02$).

Cross-sectional studies have demonstrated a negative correlation between marrow fat and bone using different measurement techniques and in different populations. However, longitudinal studies of marrow fat and bone are crucial to establish the temporal relationship of changes. Few longitudinal studies are available to date. Griffith and colleagues reported that in postmenopausal women (average age 74 years), higher levels of MAT predicted greater bone loss at the femoral neck over 4 years (63). Those with MAT levels above the median had mean bone loss of 4.7% while those below the median had mean loss of 1.6%, although the comparison was not statistically significant ($p = 0.06$). Among older adults in Iceland followed for an average of 3 years, we found that trabecular spine vBMD, spine compressive strength (derived from density and cross-sectional area), and trabecular femoral neck vBMD decreased more rapidly in those with higher BMAT in women but not in men (82). The difference in changes in trabecular spine vBMD was − 0.9% (95% CI − 1.7 to − 0.1%) for each 1 SD (~ 8%) increase in baseline MAT. In contrast, the Mayo Clinic study did not find negative correlations between baseline MAT and changes in vBMD measured with SE QCT or DE QCT (78). However, this study also reported the correlations between changes in MAT and changes in vBMD and found a negative correlation between changes in femur MAT and trabecular spine vBMD (DE QCT) ($r = -0.19$%/year, $p < 0.05$). Correlations between changes in MAT and BMD in the setting of bariatric surgery have also been reported (76). Those with increases in spine MAT had more BMD loss in spine vBMD ($r = -0.58$, $p < 0.01$), 6 months after surgery.

Marrow Fat and Fracture

There is consistent evidence from cross-sectional studies, using different methods to measure marrow adiposity, that higher MAT is associated with prevalent vertebral fracture, identified morphometrically (49, 73, 82, 83•, 84). Iliac crest biopsies were used to assess marrow adiposity in women with prevalent vertebral fracture compared with controls (63% vs 54%, $p = 0.02$) (83•). An examination of MAT in the lumbar spine and proximal femur, using MR imaging, reported higher MAT at both locations in those with prevalent vertebral fracture (73). The mean MAT at the spine was 55% and 45% ($p < 0.001$) in women with and without prevalent vertebral fracture. Among older adults (mean age 79 ± 3 years) participating in the Iceland AGES-Reykjavik study, vertebral MAT, measured by MRS, was 57% versus 54% ($p = 0.01$) comparing those with and without vertebral fracture, adjusted for spine trabecular vBMD (49). Vertebral MAT is also associated with vertebral fracture among patients with active Cushing's syndrome (84). Average vertebral MAT by MRS was 65% versus 24% ($p = 0.03$) in patients with ($N = 13$) and without ($N = 7$) vertebral fracture.

The evidence regarding clinical fracture is more limited. In a cross-sectional study comparing postmenopausal women with ($N = 36$) and without ($N = 33$) history of clinical fracture (primarily non-vertebral), vertebral MAT measured with MRS was similar between groups (44). In contrast, a recent cross-sectional study in women aged 40–70 comparing cases ($N = 77$) with a recent non-vertebral fracture and controls ($N = 226$) without fracture history reported increased odds of fracture with higher marrow adiposity index (MAI) (85). MAI was estimated from high-resolution pQCT (HR-pQCT) scans with MAI = adipose volume (AV)/ total marrow volume (TV) × relative medullary density. For each 1SD increase in MAI, the odds of fracture history increased by 3.6 (95% CI 2.2–5.9) for distal tibia MAI and 4.2 (95% CI 2.5–7.2) for distal radius MAI. To date, there are no longitudinal studies reporting the relationship between MAT and incident fracture. Such an assessment is a critical component of research efforts to determine the effects of MAT on skeletal health.

Composition of Marrow Fat and Skeletal Health

Marrow fat is composed of differing proportions of saturated and unsaturated lipids, which may be important for skeletal health. As discussed above, MRS can distinguish the relative proportion of different carbon-carbon bonds within the marrow fat. These bonds do not correspond directly to specific lipids but do provide a non-invasive estimate of the proportion of saturated versus unsaturated lipids present. Methylene protons at 1.3 ppm are considered a marker for saturated bonds while olefinic protons at 5.3 ppm are a marker for unsaturated bonds. Results are generally reported as an "unsaturation index (UI)," calculated as the ratio of the 5.3 ppm peak to all lipid peaks, as shown in Eq. (2). The UI differs by skeletal site, with higher UI at the more distal sites (86). In young adults, UI is reported to increase with age (87). However, a comparison of younger (mean age 28 years) and older (mean age 70 years) women found lower UI levels in vertebral marrow fat with older age (46). Similarly, in a study of marrow fat in the femoral head, measured with CSE-MRI, postmenopausal women had lower UI than pre-menopausal women (54). These studies on age and saturation index need further confirmation but suggest an increase in UI with skeletal maturation followed by a decrease in older age, at least for women.

A few studies have considered the relationship between marrow fat lipid composition and skeletal health. A study in Hong Kong reported that a lower proportion of unsaturated lipids are associated with lower bone density (46). Older women with osteoporotic BMD had a mean unsaturation level of 0.091 compared with 0.114 in those with normal BMD. In a study of lipid composition of marrow at the calcaneus, the ratio of saturated to unsaturated lipid was lower in those with normal BMD compared with osteopenic or osteoporotic BMD (42). In a study that included anorexic and healthy young women, higher levels of saturated lipids were associated with lower spine BMD while there was no association between saturated lipids and BMD (41).

A study using marrow fat specimens ($N = 24$), obtained by iliac crest aspiration during hip surgery, also found lower unsaturation, measured with 11.7T MRS, in the women with lower BMD (37). In contrast, in a study in Hong Kong using marrow fat specimens from elective orthopedic surgery at different skeletal sites, including the tibia ($N = 80$), proximal femur ($N = 38$), and spine ($N = 8$), analysis of fatty acid composition with gas chromatography found similar composition across levels of BMD (88). One published study has assessed unsaturated lipids and fracture, reporting that the unsaturation index was 1.7% lower (95% CI − 2.8 to − 0.5%, $p = 0.005$), in postmenopausal women with versus without prevalent fracture (44).

Importantly, these initial findings on lipid composition suggest that the different components of marrow fat have divergent associations with bone health. If these results are confirmed by further studies, it suggests that our current use of total marrow fat content in studies of marrow fat and bone, measured by either PDFF from water-fat MRI or all lipid components from MRS, may be obscuring relationships. We would predict that the same MAT content with different ratios of unsaturated and saturated fat would have different associations with BMD and with fracture. Future investigations should include separate assessment of unsaturated and saturated lipids in order to clearly distinguish the effects on bone.

Conclusions

Increasing evidence suggests a key role of marrow fat in skeletal health, affecting bone quantity and quality, although the

mechanisms of such effects remain to be fully understood. There have been significant technical advances in reliable quantification of total marrow fat content, or PDFF, using MR techniques. One exciting area with new promising results is to explore the relationship between marrow fat composition and skeletal health. However, reliable in vivo quantification of marrow fat composition remains challenging due to the heterogeneous environment of marrow with the presence of trabecular bone, compared with other adipose tissues. Non-invasive imaging techniques need to be further developed, optimized, and validated in marrow. Reliable, standardized, and automatic post-processing is also urgently needed, especially for large-scale multi-center studies that will be needed to assess the relationship between marrow fat and incident fracture. Accurate and reliable quantification of marrow fat contents and composition will help to deepen our understanding of bone-fat interaction, provide useful guidance on developing novel treatment strategy for osteoporosis with marrow fat as a treatment target, and serve as potential biomarkers and outcome measures for trials.

Compliance with Ethical Standards

Conflict of Interest The authors declare no conflict of interest.

Human and Animal Rights and Informed Consent This article does not contain any studies with human or animal subjects performed by any of the authors.

References

Papers of particular interest, published recently, have been highlighted as:
- • Of importance
- •• Of major importance

1. Schwartz AV. Marrow fat and bone: review of clinical findings. Front Endocrinol 2015;6:40. doi: https://doi.org/10.3389/fendo.2015.00040. PubMed PMID: 25870585; PubMed Central PMCID: PMC4378315.
2. Singhal V, Bredella MA. Marrow adipose tissue imaging in humans. Bone. 2019;118:69–76. Epub 2018/01/15. doi: https://doi.org/10.1016/j.bone.2018.01.009. PubMed PMID: 29331301; PubMed Central PMCID: PMCPMC6039291.
3. Rendina-Ruedy E, Rosen CJ. Bone-fat interaction. Endocrinol Metab Clin N Am 2017;46(1):41–50. doi: https://doi.org/10.1016/j.ecl.2016.09.004. PubMed PMID: 28131135; PubMed Central PMCID: PMC5300693.
4. Rosen CJ, Ackert-Bicknell C, Rodriguez JP, Pino AM. Marrow fat and the bone microenvironment: developmental, functional, and pathological implications. Crit Rev Eukaryot Gene Expr. 2009;19(2):109–24. Epub 2009/04/28. doi: 32dcc8826e8b77f6, 4bae1a4b22a0281c [pii]. PubMed PMID: 19392647; PubMed Central PMCID: PMC2674609.
5. Moerman EJ, Teng K, Lipschitz DA, Lecka-Czernik B. Aging activates adipogenic and suppresses osteogenic programs in mesenchymal marrow stroma/stem cells: the role of PPAR-gamma2 transcription factor and TGF-beta/BMP signaling pathways. Aging Cell 2004;3(6):379–389. **Epub 2004/12/01**. PubMed PMID: 15569355; PubMed Central PMCID: PMC1850101.
6. Sottile V, Seuwen K, Kneissel M. Enhanced marrow adipogenesis and bone resorption in estrogen-deprived rats treated with the PPARgamma agonist BRL49653 (rosiglitazone). Calcif Tissue Int. 2004;75(4):329–37. **Epub 2004/11/19**. https://doi.org/10.1007/s00223-004-0224-8.
7. Maurin AC, Chavassieux PM, Frappart L, Delmas PD, Serre CM, Meunier PJ. Influence of mature adipocytes on osteoblast proliferation in human primary cocultures. Bone. 2000;26(5):485–9.
8. Maurin AC, Chavassieux PM, Vericel E, Meunier PJ. Role of polyunsaturated fatty acids in the inhibitory effect of human adipocytes on osteoblastic proliferation. Bone. 2002;31(1):260–6.
9. Weisberg SP, McCann D, Desai M, Rosenbaum M, Leibel RL, Ferrante AW Jr. Obesity is associated with macrophage accumulation in adipose tissue. J Clin Invest. 2003;112(12):1796–808.
10. Hanrahan CJ, Shah LM. MRI of spinal bone marrow: part 2, T1-weighted imaging-based differential diagnosis. AJR Am J Roentgenol. 2011;197(6):1309–21. **Epub 2011/11/24**. https://doi.org/10.2214/AJR.11.7420.
11. Shah LM, Hanrahan CJ. MRI of spinal bone marrow: part I, techniques and normal age-related appearances. AJR Am J Roentgenol. 2011;197(6):1298–308. **Epub 2011/11/24**. https://doi.org/10.2214/AJR.11.7005.
12. Chan BY, Gill KG, Rebsamen SL, Nguyen JC. MR imaging of pediatric bone marrow. Radiographics. 2016;36(6):1911–30. **Epub 2016/10/12**. https://doi.org/10.1148/rg.2016160056.
13. Shen W, Scherzer R, Gantz M, Chen J, Punyanitya M, Lewis CE, et al. Relationship between MRI-measured bone marrow adipose tissue and hip and spine bone mineral density in African-American and Caucasian participants: the CARDIA study. J Clin Endocrinol Metab. 2012;97(4):1337–46. Epub 2012/02/10. doi: https://doi.org/10.1210/jc.2011-2605. PubMed PMID: 22319043; PubMed Central PMCID: PMCPMC3319176.
14. van Vucht N, Santiago R, Lottmann B, Pressney I, Harder D, Sheikh A, et al. The Dixon technique for MRI of the bone marrow. Skeletal Radiol. 2019. **Epub 2019/07/17**. doi: https://doi.org/10.1007/s00256-019-03271-4, The Dixon technique for MRI of the bone marrow.
15. Karampinos DC, Ruschke S, Dieckmeyer M, Diefenbach M, Franz D, Gersing AS, et al. Quantitative MRI and spectroscopy of bone marrow. J Magn Reson Imaging. 2018;47(2):332–53. Epub 2017/06/02. doi: https://doi.org/10.1002/jmri.25769. PubMed PMID: 28570033; PubMed Central PMCID: PMCPMC5811907.
16. Dixon WT. Simple proton spectroscopic imaging. Radiology. 1984;153(1):189–94. **Epub 1984/10/01**. https://doi.org/10.1148/radiology.153.1.6089263.
17. Reeder SB, Wen Z, Yu H, Pineda AR, Gold GE, Markl M, et al. Multicoil Dixon chemical species separation with an iterative least-squares estimation method. Magn Reson Med. 2004;51(1):35–45. **Epub 2004/01/06**. https://doi.org/10.1002/mrm.10675.
18. Hernando D, Liang ZP, Kellman P. Chemical shift-based water/fat separation: a comparison of signal models. Magn Reson Med. 2010;64(3):811–22. Epub 2010/07/02. doi: https://doi.org/10.1002/mrm.22455. PubMed PMID: 20593375; PubMed Central PMCID: PMCPMC2992842.
19. Colgan TJ, Hernando D, Sharma SD, Reeder SB. The effects of concomitant gradients on chemical shift encoded MRI. Magn Reson Med. 2017;78(2):730–8. Epub 2016/09/22. doi: https://doi.org/10.1002/mrm.26461. PubMed PMID: 27650137; PubMed Central PMCID: PMCPMC5360547.
20. Wang X, Hernando D, Reeder SB. Sensitivity of chemical shift-encoded fat quantification to calibration of fat MR spectrum. Magn Reson Med. 2016;75(2):845–51. Epub 2015/04/08. doi:

https://doi.org/10.1002/mrm.25681. PubMed PMID: 25845713; PubMed Central PMCID: PMCPMC4592785.

21. Ruschke S, Eggers H, Kooijman H, Diefenbach MN, Baum T, Haase A, et al. Correction of phase errors in quantitative water-fat imaging using a monopolar time-interleaved multi-echo gradient echo sequence. Magn Reson Med. 2017;78(3):984–96. **Epub 2016/11/01**. https://doi.org/10.1002/mrm.26485.
22. Yu H, Shimakawa A, McKenzie CA, Brodsky E, Brittain JH, Reeder SB. Multiecho water-fat separation and simultaneous R2* estimation with multifrequency fat spectrum modeling. Magn Reson Med. 2008;60(5):1122–34. Epub 2008/10/29. doi: https://doi.org/10.1002/mrm.21737. PubMed PMID: 18956464; PubMed Central PMCID: PMCPMC3070175.
23. Bydder M, Yokoo T, Hamilton G, Middleton MS, Chavez AD, Schwimmer JB, et al. Relaxation effects in the quantification of fat using gradient echo imaging. Magn Reson Imaging. 2008;26(3):347–59. Epub 2007/12/21. doi: https://doi.org/10.1016/j.mri.2007.08.012. PubMed PMID: 18093781; PubMed Central PMCID: PMCPMC2386876.
24. Karampinos DC, Yu H, Shimakawa A, Link TM, Majumdar S. T(1)-corrected fat quantification using chemical shift-based water/fat separation: application to skeletal muscle. Magn Reson Med. 2011;66(5):1312–26. Epub 2011/04/01. doi: https://doi.org/10.1002/mrm.22925. PubMed PMID: 21452279; PubMed Central PMCID: PMCPMC3150641.
25. Liu CY, McKenzie CA, Yu H, Brittain JH, Reeder SB. Fat quantification with IDEAL gradient echo imaging: correction of bias from T(1) and noise. Magn Reson Med. 2007;58(2):354–64. **Epub 2007/07/27**. https://doi.org/10.1002/mrm.21301.
26.• Karampinos DC, Melkus G, Baum T, Bauer JS, Rummeny EJ, Krug R. Bone marrow fat quantification in the presence of trabecular bone: initial comparison between water-fat imaging and single-voxel MRS. Magn Reson Med. 2014;71(3):1158–65. Epub 2013/05/10. doi: https://doi.org/10.1002/mrm.24775. PubMed PMID: 23657998; PubMed Central PMCID: PMCPMC3759615. **This study presented a thorough evaluation of performance of water-fat imaging in quantifying bone marrow fat fraction, in the presence of trabecular bone and using single voxel MRS as references.**
27. Arentsen L, Yagi M, Takahashi Y, Bolan PJ, White M, Yee D, et al. Validation of marrow fat assessment using noninvasive imaging with histologic examination of human bone samples. Bone. 2015;72:118–22. Epub 2014/12/03. doi: https://doi.org/10.1016/j.bone.2014.11.002. PubMed PMID: 25460181; PubMed Central PMCID: PMCPMC4282942.
28. Ruschke S, Pokorney A, Baum T, Eggers H, Miller JH, Hu HH, et al. Measurement of vertebral bone marrow proton density fat fraction in children using quantitative water-fat MRI. MAGMA. 2017;30(5):449–60. **Epub 2017/04/07**. https://doi.org/10.1007/s10334-017-0617-0.
29. Gee CS, Nguyen JT, Marquez CJ, Heunis J, Lai A, Wyatt C, et al. Validation of bone marrow fat quantification in the presence of trabecular bone using MRI. J Magn Reson Imaging. 2015;42(2):539–44. Epub 2014/11/27. doi: https://doi.org/10.1002/jmri.24795. PubMed PMID: 25425074; PubMed Central PMCID: PMCPMC4442769.
30. Baum T, Yap SP, Dieckmeyer M, Ruschke S, Eggers H, Kooijman H, et al. Assessment of whole spine vertebral bone marrow fat using chemical shift-encoding based water-fat MRI. J Magn Reson Imaging. 2015;42(4):1018–23. **Epub 2015/02/03**. https://doi.org/10.1002/jmri.24854.
31. Li G, Xu Z, Yuan W, Chang S, Chen Y, Calimente H, et al. Short- and midterm reproducibility of marrow fat measurements using mDixon imaging in healthy postmenopausal women. Skelet Radiol. 2016;45(10):1385–90. **Epub 2016/08/10**. https://doi.org/10.1007/s00256-016-2448-x.
32. Zhang Y, Zhou Z, Wang C, Cheng X, Wang L, Duanmu Y, et al. Reliability of measuring the fat content of the lumbar vertebral marrow and paraspinal muscles using MRI mDIXON-Quant sequence. Diagn Interv Radiol. 2018;24(5):302–7. Epub 2018/09/05. doi: https://doi.org/10.5152/dir.2018.17323. PubMed PMID: 30179158; PubMed Central PMCID: PMCPMC6135056.
33.• Schmeel FC, Vomweg T, Traber F, Gerhards A, Enkirch SJ, Faron A, et al. Proton density fat fraction MRI of vertebral bone marrow: accuracy, repeatability, and reproducibility among readers, field strengths, and imaging platforms. J Magn Reson Imaging. 2019. Epub 2019/04/14. doi: https://doi.org/10.1002/jmri.26748. **This study reported the accuracy (using measures from MR spectroscopy as references) and precision of MRI-determined vertebral bone marrow proton density fat fraction (PDFF) among different readers and across different field strengths and imaging manufacturers.**
34. Hamilton G, Middleton MS, Bydder M, Yokoo T, Schwimmer JB, Kono Y, et al. Effect of PRESS and STEAM sequences on magnetic resonance spectroscopic liver fat quantification. J Magn Reson Imaging. 2009;30(1):145–52. Epub 2009/06/27. doi: https://doi.org/10.1002/jmri.21809. PubMed PMID: 19557733; PubMed Central PMCID: PMCPMC2982807.
35. Guillen MD, Ruiz A. H-1 nuclear magnetic resonance as a fast tool for determining the composition of acyl chains in acylglycerol mixtures. Eur J Lipid Sci Tech. 2003;105(9):502–7. doi: https://doi.org/10.1002/ejlt.200300799. PubMed PMID: WOS:000185589500005.
36. Ren J, Dimitrov I, Sherry AD, Malloy CR. Composition of adipose tissue and marrow fat in humans by 1H NMR at 7 Tesla. J Lipid Res. 2008;49(9):2055–62. **Epub 2008/05/30 doi: D800010-JLR200 [pii]**.
37. 1194/jlr.D800010-JLR200. PubMed PMID: 18509197; PubMed Central PMCID: PMC2515528.
38. Li X, Shet K, Xu K, Rodriguez JP, Pino AM, Kurhanewicz J, et al. Unsaturation level decreased in bone marrow fat of postmenopausal women with low bone density using high resolution magic angle spinning (HRMAS) (1)H NMR spectroscopy. Bone. 2017;105:87–92. Epub 2017/08/22. doi: https://doi.org/10.1016/j.bone.2017.08.014. PubMed PMID: 28823880; PubMed Central PMCID: PMCPMC5650928.
39. De Bisschop E, Luypaert R, Louis O, Osteaux M. Fat fraction of lumbar bone marrow using in vivo proton nuclear magnetic resonance spectroscopy. Bone. 1993;14(2):133–6. **Epub 1993/03/01**. https://doi.org/10.1016/8756-3282(93)90239-7.
40. Liney G, Bernard C, Manton D, Turnbull L, Langton C. Age, gender, and skeletal variation in bone marrow composition: a preliminary study at 3.0 Tesla. J Magn Reson Imaging. 2007;26(3):787–93.
41. Kugel H, Jung C, Schulte O, Heindel W. Age- and sex-specific differences in the 1H-spectrum of vertebral bone marrow. J Magn Reson Imaging. 2001;13(2):263–8. **Epub 2001/02/13**. https://doi.org/10.1002/1522-2586(200102)13:2<263::AID-JMRI1038>3.0.CO;2-M **[pii]**.
42. Bredella MA, Fazeli PK, Daley SM, Miller KK, Rosen CJ, Klibanski A, et al. Marrow fat composition in anorexia nervosa. Bone. 2014;66:199–204. Epub 2014/06/24. doi: https://doi.org/10.1016/j.bone.2014.06.014. PubMed PMID: 24953711; PubMed Central PMCID: PMCPmc4125432.
43. Di Pietro G, Capuani S, Manenti G, Vinicola V, Fusco A, Baldi J, et al. Bone marrow lipid profiles from peripheral skeleton as potential biomarkers for osteoporosis: a 1H-MR spectroscopy study. Acad Radiol. 2016;23(3):273–83. **Epub 2016/01/18**. https://doi.org/10.1016/j.acra.2015.11.009.
44. Li X, Kuo D, Schafer AL, Porzig A, Link TM, Black D, Schwartz AV Quantification of vertebral bone marrow fat content using 3 Tesla MR spectroscopy: reproducibility, vertebral variation, and applications in osteoporosis. J Magn Reson Imaging 2011;33(4):

974–979. **Epub 2011/03/31**. doi: https://doi.org/10.1002/jmri.22489. PubMed PMID: 21448966; PubMed Central PMCID: PMC3072841.

45. Patsch JM, Li X, Baum T, Yap SP, Karampinos DC, Schwartz AV, Link TM Bone marrow fat composition as a novel imaging biomarker in postmenopausal women with prevalent fragility fractures. J Bone Miner Res 2013;28(8):1721–1728. doi: https://doi.org/10.1002/jbmr.1950. PubMed PMID: 23558967; PubMed Central PMCID: PMC3720702.
46. Griffith J, Yeung D, Antonio G, Lee F, Hong A, Wong S, et al. Vertebral bone mineral density, marrow perfusion, and fat content in healthy men and men with osteoporosis: dynamic contrast-enhanced MR imaging and MR spectroscopy. Radiology. 2005;236(3):945–51.
47. Yeung D, Griffith J, Antonio G, Lee F, Woo J, Leung P. Osteoporosis is associated with increased marrow fat content and decreased marrow fat unsaturation: a proton MR spectroscopy study. J Magn Reson Imaging. 2005;22(2):279–85.
48.• Xu K, Sigurdsson S, Gudnason V, Hue T, Schwartz A, Li X. Reliable quantification of marrow fat content and unsaturation level using in vivo MR spectroscopy. Magn Reson Med. 2018;79(3):1722–9. Epub 2017/07/18. doi: https://doi.org/10.1002/mrm.26828. PubMed PMID: 28714169; PubMed Central PMCID: PMCPMC5930928: **This study developed a novel, fully automated technique for reliable quantification of bone marrow fat content and composition (unsaturation level) using in vivo MR spectroscopy (MRS), which can be potentially used in larger scale clinical trials.**
49. Dieckmeyer M, Ruschke S, Cordes C, Yap SP, Kooijman H, Hauner H, et al. The need for T(2) correction on MRS-based vertebral bone marrow fat quantification: implications for bone marrow fat fraction age dependence. NMR Biomed. 2015;28(4):432–9. **Epub 2015/02/17**. https://doi.org/10.1002/nbm.3267.
50. Schwartz AV, Sigurdsson S, Hue TF, Lang TF, Harris TB, Rosen CJ, Vittinghoff E, Siggeirsdottir K, Sigurdsson G, Oskarsdottir D, Shet K, Palermo L, Gudnason V, Li X Vertebral bone marrow fat associated with lower trabecular BMD and prevalent vertebral fracture in older adults. J Clin Endocrinol Metab 2013;98(6):2294–2300. **Epub 2013/04/05**. doi: https://doi.org/10.1210/jc.2012-3949. PubMed PMID: 23553860; PubMed Central PMCID: PMC3667265.
51. Singhal V, Miller KK, Torriani M, Bredella MA. Short- and long-term reproducibility of marrow adipose tissue quantification by 1H-MR spectroscopy. Skeletal Radiol. 2016;45(2):221–5. Epub 2015/11/14. doi: https://doi.org/10.1007/s00256-015-2292-4. PubMed PMID: 26563561; PubMed Central PMCID: PMCPMC4864977.
52. Griffith JF, Yeung DK, Chow SK, Leung JC, Leung PC. Reproducibility of MR perfusion and (1)H spectroscopy of bone marrow. J Magn Reson Imaging. 2009;29(6):1438–42. **Epub 2009/05/28**. https://doi.org/10.1002/jmri.21765.
53.• Peterson P, Mansson S. Simultaneous quantification of fat content and fatty acid composition using MR imaging. Magn Reson Med. 2013;69(3):688-97. Epub 2012/04/26. doi: https://doi.org/10.1002/mrm.24297. PubMed PMID: 22532403: **This study developed a novel image reconstruction technique that allows quantifying both fat content and fatty acid composition using fat-water imaging. The results were validated in phantoms and feasibility of in vivo imaging was demonstrated.**
54. Leporq B, Lambert SA, Ronot M, Vilgrain V, Van Beers BE. Quantification of the triglyceride fatty acid composition with 3.0 T MRI. NMR Biomed. 2014;27(10):1211–21. **Epub 2014/08/16**. https://doi.org/10.1002/nbm.3175.
55. Martel D, Leporq B, Bruno M, Regatte RR, Honig S, Chang G. Chemical shift-encoded MRI for assessment of bone marrow adipose tissue fat composition: pilot study in premenopausal versus postmenopausal women. Magn Reson Imaging. 2018;53:148–55. **Epub 2018/07/15**. https://doi.org/10.1016/j.mri.2018.07.001.
56. Martel D, Leporq B, Saxena A, Belmont HM, Turyan G, Honig S, et al. 3T chemical shift-encoded MRI: Detection of altered proximal femur marrow adipose tissue composition in glucocorticoid users and validation with magnetic resonance spectroscopy. J Magn Reson Imaging. 2019;50(2):490–6. Epub 2018/12/15. doi: https://doi.org/10.1002/jmri.26586. PubMed PMID: 30548522; PubMed Central PMCID: PMCPMC6675589.
57. Tufts LS, Shet K, Liang F, Majumdar S, Li X. Quantification of bone marrow water and lipid composition in anterior cruciate ligament-injured and osteoarthritic knees using three-dimensional magnetic resonance spectroscopic imaging. Magn Reson Imaging 2016;34(5):632–637. doi: https://doi.org/10.1016/j.mri.2015.12.034. PubMed PMID: 26723848; PubMed Central PMCID: PMC4860057.
58. Biffar A, Dietrich O, Sourbron S, Duerr HR, Reiser MF, Baur-Melnyk A. Diffusion and perfusion imaging of bone marrow. Eur J Radiol. 2010;76(3):323–8. **Epub 2010/04/13**. https://doi.org/10.1016/j.ejrad.2010.03.011.
59. Dietrich O, Geith T, Reiser MF, Baur-Melnyk A. Diffusion imaging of the vertebral bone marrow. NMR Biomed. 2017;30(3). **Epub 2015/06/27**. doi: https://doi.org/10.1002/nbm.3333.
60. Shih TT, Liu HC, Chang CJ, Wei SY, Shen LC, Yang PC. Correlation of MR lumbar spine bone marrow perfusion with bone mineral density in female subjects. Radiology. 2004;233(1):121–8. **Epub 2004/08/20**. https://doi.org/10.1148/radiol.2331031509.
61. Griffith JF, Yeung DK, Antonio GE, Wong SY, Kwok TC, Woo J, et al. Vertebral marrow fat content and diffusion and perfusion indexes in women with varying bone density: MR evaluation. Radiology. 2006;241(3):831–8. **Epub 2006/10/21**. https://doi.org/10.1148/radiol.2413051858.
62. Griffith JF, Yeung DK, Tsang PH, Choi KC, Kwok TC, Ahuja AT, et al. Compromised bone marrow perfusion in osteoporosis. Journal of bone and mineral research : the official journal of the American Society for Bone and Mineral Research. 2008;23(7):1068–75. **Epub 2008/02/28**. https://doi.org/10.1359/jbmr.080233.
63. Wang YX, Griffith JF, Kwok AW, Leung JC, Yeung DK, Ahuja AT, et al. Reduced bone perfusion in proximal femur of subjects with decreased bone mineral density preferentially affects the femoral neck. Bone. 2009;45(4):711–5. **Epub 2009/06/27**. https://doi.org/10.1016/j.bone.2009.06.016.
64.• Griffith JF, Yeung DK, Leung JC, Kwok TC, Leung PC. Prediction of bone loss in elderly female subjects by MR perfusion imaging and spectroscopy. Eur Radiol. 2011;21(6):1160–9. Epub 2011/01/13. doi: https://doi.org/10.1007/s00330-010-2054-6. **This study demonstrated the potential predict capability of baseline marrow composition to longitudinal bone loss. The study reported elderly female subjects with reduced perfusion indices at baseline had inreased femoral neck bone loss (measured by DXA) at 4 years. Selected perfusion indices and marrow fat content have a moderate to high sensitivity in discrimatinating between fast and slow bone losers.**
65. Biffar A, Schmidt GP, Sourbron S, D'Anastasi M, Dietrich O, Notohamiprodjo M, et al. Quantitative analysis of vertebral bone marrow perfusion using dynamic contrast-enhanced MRI: initial results in osteoporotic patients with acute vertebral fracture. J Magn Reson Imaging. 2011;33(3):676–83. **Epub 2011/05/13**. https://doi.org/10.1002/jmri.22497.
66. Lasbleiz J, Le Ster C, Guillin R, Saint-Jalmes H, Gambarota G. Measurements of diffusion and perfusion in vertebral bone marrow using intravoxel incoherent motion (IVIM) with multishot, readout-segmented (RESOLVE) echo-planar imaging. J Magn Reson Imaging. 2019;49(3):768–76. **Epub 2018/09/09**. https://doi.org/10.1002/jmri.26270.

67. Hillengass J, Stieltjes B, Bauerle T, McClanahan F, Heiss C, Hielscher T, et al. Dynamic contrast-enhanced magnetic resonance imaging (DCE-MRI) and diffusion-weighted imaging of bone marrow in healthy individuals. Acta Radiol. 2011;52(3):324–30. **Epub 2011/04/19**. https://doi.org/10.1258/ar.2010.100366.
68. Yeung DK, Wong SY, Griffith JF, Lau EM. Bone marrow diffusion in osteoporosis: evaluation with quantitative MR diffusion imaging. J Magn Reson Imaging. 2004;19(2):222–8. **Epub 2004/01/28**. https://doi.org/10.1002/jmri.10453.
69. Herrmann J, Krstin N, Schoennagel BP, Sornsakrin M, Derlin T, Busch JD, et al. Age-related distribution of vertebral bone-marrow diffusivity. Eur J Radiol. 2012;81(12):4046–9. **Epub 2012/09/29**. https://doi.org/10.1016/j.ejrad.2012.03.033.
70. Hatipoglu HG, Selvi A, Ciliz D, Yuksel E. Quantitative and diffusion MR imaging as a new method to assess osteoporosis. AJNR Am J Neuroradiol. 2007;28(10):1934–7. **Epub 2007/10/02**. https://doi.org/10.3174/ajnr.A0704.
71. Tang GY, Lv ZW, Tang RB, Liu Y, Peng YF, Li W, et al. Evaluation of MR spectroscopy and diffusion-weighted MRI in detecting bone marrow changes in postmenopausal women with osteoporosis. Clin Radiol. 2010;65(5):377–81. **Epub 2010/04/13**. https://doi.org/10.1016/j.crad.2009.12.011.
72. Ueda Y, Miyati T, Ohno N, Motono Y, Hara M, Shibamoto Y, et al. Apparent diffusion coefficient and fractional anisotropy in the vertebral bone marrow. J Magn Reson Imaging. 2010;31(3):632–5. **Epub 2010/02/27**. https://doi.org/10.1002/jmri.22073.
73. Meunier P, Aaron J, Edouard C, Vignon G. Osteoporosis and the replacement of cell populations of the marrow by adipose tissue. A quantitative study of 84 iliac bone biopsies. Clin Orthop Relat Res. 1971;80:147–54.
74. Wehrli FW, Hopkins JA, Hwang SN, Song HK, Snyder PJ, Haddad JG. Cross-sectional study of osteopenia with quantitative MR imaging and bone densitometry. Radiology. 2000;217(2):527–38. **Epub 2000/11/04**. https://doi.org/10.1148/radiology.217.2.r00nv20527.
75. Shen W, Chen J, Punyanitya M, Shapses S, Heshka S, Heymsfield SB. MRI-measured bone marrow adipose tissue is inversely related to DXA-measured bone mineral in Caucasian women. Osteoporosis international : a journal established as result of cooperation between the European Foundation for Osteoporosis and the National Osteoporosis Foundation of the USA. 2007;18(5):641–7.
76. Baum T, Yap SP, Karampinos DC, Nardo L, Kuo D, Burghardt AJ, Masharani UB, Schwartz AV, Li X, Link TM Does vertebral bone marrow fat content correlate with abdominal adipose tissue, lumbar spine bone mineral density, and blood biomarkers in women with type 2 diabetes mellitus? J Magn Reson Imaging 2012;35(1):117–124. doi: https://doi.org/10.1002/jmri.22757. PubMed Central PMCID: PMC3245661.
77. Kim TY, Schwartz AV, Li X, Xu K, Black DM, Petrenko DM, et al. Bone marrow fat changes after gastric bypass surgery are associated with loss of bone mass. Journal of bone and mineral research : the official journal of the American Society for Bone and Mineral Research. 2017;32(11):2239–47. Epub 2017/08/10. doi: https://doi.org/10.1002/jbmr.3212. PubMed PMID: 28791737; PubMed Central PMCID: PMCPmc5685913.
78. Ivaska KK, Huovinen V, Soinio M, Hannukainen JC, Saunavaara V, Salminen P, et al. Changes in bone metabolism after bariatric surgery by gastric bypass or sleeve gastrectomy. Bone. 2017;95:47–54. **Epub 2016/11/08**. https://doi.org/10.1016/j.bone.2016.11.001.
79. Sfeir JG, Drake MT, Atkinson EJ, Achenbach SJ, Camp JJ, Tweed AJ, et al. Evaluation of cross-sectional and longitudinal changes in volumetric bone mineral density in postmenopausal women using single- versus dual-energy quantitative computed tomography. Bone. 2018;112:145–52. Epub 2018/04/29. doi: https://doi.org/10.1016/j.bone.2018.04.023. PubMed PMID: 29704696; PubMed Central PMCID: PMCPmc5970096.
80. Glüer CC, Reiser UJ, Davis CA, Rutt BK, Genant HK. Vertebral mineral determination by quantitative computed tomography (QCT): accuracy of single and dual energy measurements. J Comput Assist Tomogr. 1988;12:242–58.
81. Bredella MA, Daley SM, Kalra MK, Brown JK, Miller KK, Torriani M. Marrow adipose tissue quantification of the lumbar spine by using dual-energy CT and single-voxel (1)H MR spectroscopy: a feasibility study. Radiology. 2015;277(1):230–5. Epub 2015/05/20. doi: https://doi.org/10.1148/radiol.2015142876. PubMed PMID: 25988401; PubMed Central PMCID: PMCPmc4613879.
82. Singhal V, Torre Flores LP, Stanford FC, Toth AT, Carmine B, Misra M, et al. Differential associations between appendicular and axial marrow adipose tissue with bone microarchitecture in adolescents and young adults with obesity. Bone. 2018;116:203–6. Epub 2018/08/15. doi: https://doi.org/10.1016/j.bone.2018.08.009. PubMed PMID: 30107255; PubMed Central PMCID: PMCPmc6158042.
83.• Woods GN, Ewing SK, Sigurdsson S, Kado DM, Eiriksdottir G, Gudnason V, et al. Greater bone marrow adiposity predicts bone loss in older women. J Bone Miner Res. 2019. Epub 2019/10/17. doi: https://doi.org/10.1002/jbmr.3895. **This longitudinal study demonstrated that the higher levels of marrow fat, as measured by MRS, predict greater loss of trabecular bone at the spine and femoral neck, and greater loss of spine compressive strength, as measured by QCT, in older women.**
84. Justesen J, Stenderup K, Ebbesen EN, Mosekilde L, Steiniche T, Kassem M. Adipocyte tissue volume in bone marrow is increased with aging and in patients with osteoporosis. Biogerontology. 2001;2(3):165–71.
85. Ferrau F, Giovinazzo S, Messina E, Tessitore A, Vinci S, Mazziotti G, et al. High bone marrow fat in patients with Cushing's syndrome and vertebral fractures. Endocrine. 2019. **Epub 2019/08/04**. doi: https://doi.org/10.1007/s12020-019-02034-4.
86. Zebaze R, Osima M, Bui M, Lukic M, Wang X, Ghasem-Zadeh A, et al. Adding marrow adiposity and cortical porosity to femoral neck areal bone mineral density improves the discrimination of women with nonvertebral fractures from controls. Journal of bone and mineral research : the official journal of the American Society for Bone and Mineral Research. 2019;34(8):1451–60. **Epub 2019/03/19**. https://doi.org/10.1002/jbmr.3721.
87. Scheller EL, Doucette CR, Learman BS, Cawthorn WP, Khandaker S, Schell B, Wu B, Ding SY, Bredella MA, Fazeli PK, Khoury B, Jepsen KJ, Pilch PF, Klibanski A, Rosen CJ, MacDougald O Region-specific variation in the properties of skeletal adipocytes reveals regulated and constitutive marrow adipose tissues. Nat Commun 2015;6:7808. doi: https://doi.org/10.1038/ncomms8808. PubMed PMID: 26245716; PubMed Central PMCID: PMC4530473.
88. Huovinen V, Viljakainen H, Hakkarainen A, Saukkonen T, Toiviainen-Salo S, Lundbom N, et al. Bone marrow fat unsaturation in young adults is not affected by present or childhood obesity, but increases with age: a pilot study. Metab Clin Exp. 2015;64(11):1574–81. **Epub 2015/09/22**. https://doi.org/10.1016/j.metabol.2015.08.014.